

UNIVERSIDAD SAN FRANCISCO DE QUITO USFQ

Colegio de Ciencias e Ingenierías

**Optimization of an SSW device for non-destructive measurement
of Young's modulus**

María José Torres Constante

Ingeniería Civil

Trabajo de fin de carrera presentado como
requisito para la obtención del título de
Ingeniero Civil

Quito, 30 de noviembre de 2024

UNIVERSIDAD SAN FRANCISCO DE QUITO USFQ

Colegio de Ciencias e Ingenierías

**HOJA DE CALIFICACIÓN
DE TRABAJO DE FIN DE CARRERA**

**Optimization of an SSW device for non-destructive measurement
of Young's modulus**

María José Torres Constante

Nombre del profesor, Título académico

Juan Pablo Villacreses, PhD.

Quito, 30 de noviembre de 2024

© DERECHOS DE AUTOR

Por medio del presente documento certifico que he leído todas las Políticas y Manuales de la Universidad San Francisco de Quito USFQ, incluyendo la Política de Propiedad Intelectual USFQ, y estoy de acuerdo con su contenido, por lo que los derechos de propiedad intelectual del presente trabajo quedan sujetos a lo dispuesto en esas Políticas.

Asimismo, autorizo a la USFQ para que realice la digitalización y publicación de este trabajo en el repositorio virtual, de conformidad a lo dispuesto en la Ley Orgánica de Educación Superior del Ecuador.

Nombres y apellidos: María José Torres Constante

Código: 00215651

Cédula de identidad: 1104732035

Lugar y fecha: Quito, 30 de noviembre de 2024

ACLARACIÓN PARA PUBLICACIÓN

Nota: El presente trabajo, en su totalidad o cualquiera de sus partes, no debe ser considerado como una publicación, incluso a pesar de estar disponible sin restricciones a través de un repositorio institucional. Esta declaración se alinea con las prácticas y recomendaciones presentadas por el Committee on Publication Ethics COPE descritas por Barbour et al. (2017) Discussion document on best practice for issues around theses publishing, disponible en <http://bit.ly/COPETheses>.

UNPUBLISHED DOCUMENT

Note: The following capstone project is available through Universidad San Francisco de Quito USFQ institutional repository. Nonetheless, this project – in whole or in part – should not be considered a publication. This statement follows the recommendations presented by the Committee on Publication Ethics COPE described by Barbour et al. (2017) Discussion document on best practice for issues around theses publishing available on <http://bit.ly/COPETheses>.

ABSTRACT

This research focuses on modifying a solitary strain wave device for enhanced measurements on soft soil materials by incorporating a thin polylactic acid (PLA) plate. Traditionally, the device operates on the principle of non-linear wave propagation through a chain of spheres, using the time of flight (TOF) between incident and reflected waves to compute the Young's modulus of tested samples. The introduction of the PLA plate enhances the device's performance by distributing the contact force over a larger area, which is particularly beneficial for soft soils. The study is conducted in three stages: modifying the Hertz contact equation through finite element analysis, solving dynamic equilibrium equations and testing the device on control samples with known properties and soil samples. The results indicate that the PLA plate effectively reduces plastic deformations and improves TOF measurement accuracy, supporting the potential of TOF as a reliable parameter for multiple applications.

Key words: non-linear solitary waves, soil Young's modulus, compaction control, non-destructive test devices

TABLE OF CONTENTS

| | |
|---------------------------------|----|
| INTRODUCTION | 9 |
| THEORICAL CONSIDERATIONS | 11 |
| MATERIALS AND METHODOLOGY | 13 |
| RESULTS AND DISCUSSION | 18 |
| CONCLUSIONS | 24 |
| BIBLIOGRAPHY | 25 |

INDEX OF TABLES

| | |
|--|----|
| Table 1-FEM sets..... | 14 |
| Table 2-Material Properties of Control samples and experimental measurements. | 16 |
| Table 3- Measured Young modulus using de Solitary strain wave device..... | 23 |

INDEX OF FIGURES

| | |
|---|----|
| Figure 1-Modified solitary strain wave device. | 12 |
| Figure 2- Finite element model setup. | 14 |
| Figure 3-Finite element model for sphere-plate-soil interaction. | 15 |
| Figure 4-Solitary-Strain wave device setup. | 17 |
| Figure 5-Indentation response of the sphere using a range of plate materials..... | 18 |
| Figure 6-Indentation response of 0.0, 0.2, 0.4 and 1.0 mm PLA plates thicknesses. | 19 |
| Figure 7-Fits of the FEM results to the proposed equation. | 19 |
| Figure 8-Relationship between Time of flight (TOF) and the Young modulus of the tested material..... | 20 |
| Figure 9-Unmodified and modified solitary strain wave device. | 21 |
| Figure 10-Comparison of measured and simulated values on rigid foam samples. | 22 |

INTRODUCTION

The accurate measurement of soil elastic properties, particularly Young's modulus, is essential in geotechnical applications, influencing a wide range of fields such as road construction, foundation design, and soil stability analysis. These properties directly affect the behavior of soils under load, shaping the performance and longevity of infrastructure. Understanding the relationship between soil stiffness, compaction, load-bearing capacity, and material behavior is crucial for designing resilient structures and ensuring their stability over time. Reliable and precise measurement of Young's modulus enables engineers to optimize design parameters and predict soil performance in both laboratory and field settings.

While laboratory testing on undisturbed soil samples provides critical insights, translating these measurements to field conditions presents challenges due to differences in testing methods used in each setting (Carol, Bernardo, & Luc, 2010). For instance, in road construction, mechanistic pavement designs are based on material modulus, but field compaction is often evaluated through density measurements (Belcher, 1952). This disparity underscores the need for alternative methods that can bridge the gap between laboratory tests and field verification. The solitary strain wave device, which utilizes strain wave propagation through a chain of packed spheres, shows promise in addressing these challenges. The device generates a wave that travels through the surveyed medium, producing a reflected wave, and the Time of Flight (TOF) between these waves is measured. This TOF is related to the stiffness of the medium, offering a potential method for assessing soil properties in situ. Although previous studies have successfully applied this device to rocks and compacted materials (Villacreses, Caicedo, Caro,

& Yépez, 2021), its application to softer soils remains underexplored, presenting an opportunity for further research.

While numerical models have been developed to correlate TOF with material properties such as Young's modulus, many of these models assume purely elastic behavior and neglect plastic deformations (Yang, Silvestro, Khatri, De Nardo, & Daraio, 2011). This research seeks to refine the Hertz contact equation by incorporating a thin plate between the device's final element and the surveyed medium. By developing new relationships between TOF, Young's modulus, and soil density, the modified device could provide more accurate measurements, particularly for softer soils.

This study is structured in three stages: (1) modifying the Hertz contact equation using finite element analysis to account for the thin plate, (2) solving the dynamic equilibrium equations for the device chain and establishing a relationship between Young's modulus and TOF, (3) testing the relationship with rigid polyurethane foam and soil samples. This research aims to enhance geotechnical testing techniques, providing more accurate insights into soil properties and facilitating better field applications.

THEORETICAL CONSIDERATIONS

The SSW device operates based on the theory of nonlinear solitary waves, as described by (Nesterenko, 2013) and (Rizzo & Li, 2017). Its primary function is to generate and propagate a wave along a chain of steel spheres held vertically over a soil specimen. The wave reflects upon interaction with the surveyed medium, and the time elapsed between the incident and reflected waves (Time of Flight, TOF) is used to determine the Young's modulus of the material.

This relies on solving a system of dynamic equilibrium equations that describe the forces within the chain and the medium. These equations are derived from Hertz's contact law (Hertz, 1882) and use contact mechanics theory (Popov, 2010) (Sneddon, 1965) (Zhai, Gan, Hanaor, Proust, & Retraint, 2016). In the original design, the system modeled interactions as sphere-sphere contact and sphere-flat surface contact.

However, a limitation was identified in previous research (Villacreses, Caicedo, Caro, & Yépez, 2021), identifying that soft soils lack the stiffness to withstand the high stress induced by the device, leading to inaccuracies in measurements. To address this and reduce the plastic deformations induced by the device, a plate is considered as a modification in the design to distribute the forces exerted.

The modified device, illustrated in Figure 1, incorporates the plate between the lowest sphere and the soil surface. This change preserves the principle of dynamic equilibrium while refining the force distribution. The interaction forces between the spheres, sensor, PLA plate, and medium are modeled using the same dynamic differential equations from (Villacreses, Caicedo, Caro, & Yépez, 2021), adapted for the modified contact scenario for the last contact equation. By capturing the TOF from the incident and reflected waves, the system of equations describing the chain's dynamics and the medium's response can be resolved. This allows the

Young's modulus of the soil to be calculated with greater accuracy, particularly for soft soils, where the modification mitigates plastic deformation and enhances the reliability of the device. Therefore, in the following sections, a detailed methodology will be developed considering this theoretical basis to implement the modification on the SSW device.

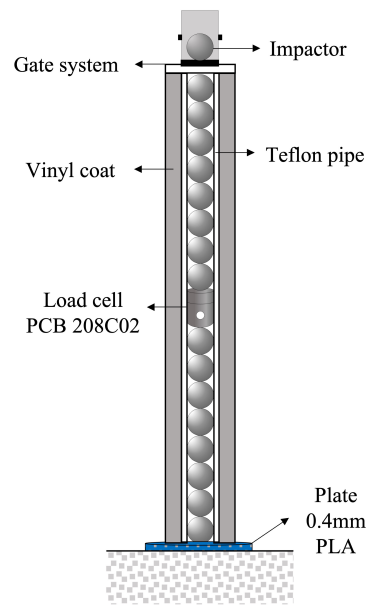


Figure 1-Modified solitary strain wave device.

MATERIALS AND METHODOLOGY

The research consisted of three stages. The first stage used finite element simulations to evaluate the impact of incorporating a thin, flexible plate into the contact mechanics. Assessing the feasibility of plates made from different materials and thicknesses. The second stage employed finite difference simulations to analyze how this modification influenced the propagation of a nonlinear solitary strain wave. The final stage involved experimental validation, where the modified device was tested on control samples with known elastic properties.

Stage I: Finite Element Simulation

In Stage I, finite element modeling (FEM) in ABAQUS was used to study the effect of introducing a plate under the last device element on the contact equation. The axisymmetric two-dimensional model analyzed reaction forces at the interface between the last device element and the sample. Boundary conditions were defined to minimize edge effects: the right boundary restricted horizontal displacement, while the bottom boundary restricted both horizontal and vertical displacements. The indenter, modeled as a rigid body with a 9.53 mm radius, applied variable displacements at a top node, and the resulting reaction force was recorded. The soil was modeled as an elastic, weightless material, and the interfaces were assumed frictionless, consistent with prior studies. (Rizzo & Li, 2017) (Popov, 2010) (Ni, Rizzo, Yang, Katri, & Daraio, 2012)

The FEM model comprised three parts: a rigid indenter meshed with four-node elements, a thin plate divided into 2,000 four-node quadrilateral elements, and a soil sample meshed with 25,000 elements, with finer mesh sizes near the plate-sphere interface. Static analysis was performed with 1,000 incremental steps, each increasing displacement by 0.0001 mm. The next figure shows the schematic of the finite element model setup.

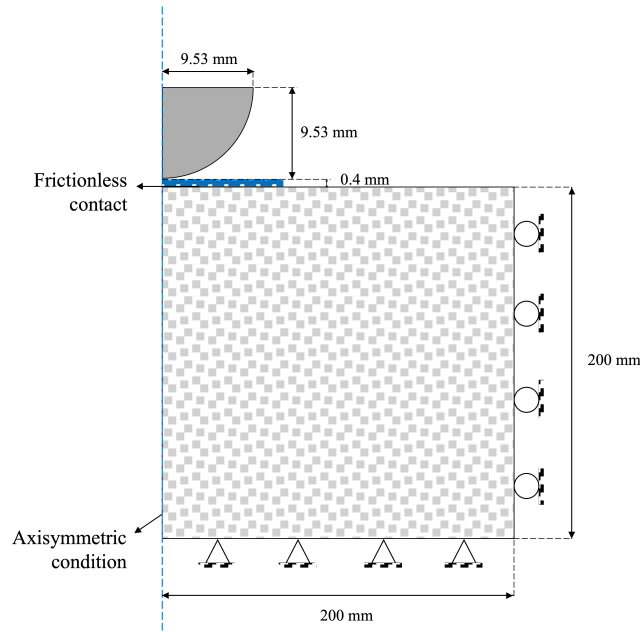


Figure 2- Finite element model setup.

Three sets of FEM simulations were conducted. The first set varied plate material (Aluminum: 10 MPa, PLA: 100 MPa, Steel A36: 210 MPa) while maintaining a constant thickness of 0.4 mm. The second set investigated the effect of PLA plates of varying thicknesses (0.1, 0.2, 0.4, and 1 mm). The third set examined the influence of soil Young's modulus (ranging from 10 MPa to 1,000 MPa) while keeping plate material and thickness constant. The goal of the first two sets was to determine a plate configuration that minimized deviations from the Hertzian contact law. The third set analyzed the sensitivity of these deviations to variations in soil stiffness. These sets are explained in the following table:

| Set | Varied Parameter | Constant Parameters | Values Explored |
|-----|----------------------------|--|--|
| 1 | Plate Material | Thickness (0.4 mm) | - Aluminum: 10 MPa - Polylactic Acid (PLA): 100 MPa - Steel A36: 210 MPa |
| 2 | Plate Thickness | Material (PLA) | - 0.2 mm - 0.4 mm - 1 mm |
| 3 | Soil Elastic Young Modulus | Plate Material (PLA) Thickness (0.4 mm) | - 10 MPa to 1000 MPa constantly increasing by 10 MPa |

Table 1-FEM sets.

Force and displacement data from the simulations were used to compute a coefficient via least squares regression, modifying the Hertz contact equation with an additional term. This coefficient quantified the deviation introduced by the plate and its influence on the ideal sphere-soil interaction. Finally, FEM simulations explored how the soil Young's modulus affected this coefficient, providing insight into the plate's behavior across a range of soil conditions. The next figure shows a schematic representation of the interaction-model:

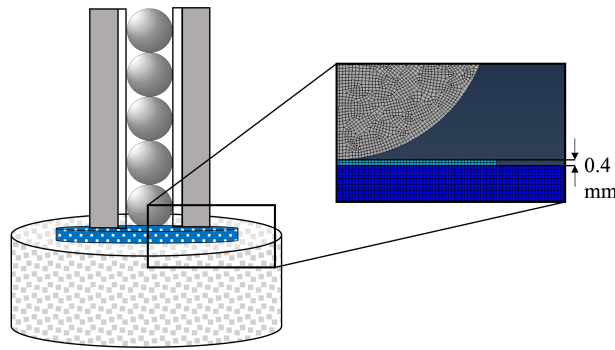


Figure 3-Finite element model for sphere-plate-soil interaction.

Stage II: Finite difference simulation

The finite element results from Stage I were used to modify the motion equation of the device's last element, based on the formulation by (Villacreses, Caicedo, Caro, & Yépez, 2021). To explore the modification of Hertz contact equation when a flexible element is introduced, a constant $K(E)$, was introduced to account for its influence. Using a finite difference approach, an explicit solution was derived to relate the soil's Young's modulus to the time of flight (TOF). The TOF, measured as the peak-to-peak distance, represents the duration between the incident and reflected wave in a specific element of the particle chain. The central element, containing the dynamic sensor, was used for these measurements.

This relationship between TOF and Young's modulus was developed to enable experimental estimations using the real device. Simulations were conducted for Poisson ratios of 0.1, 0.3, and 0.5, with the soil Young's modulus ranging from 10 MPa to 1,000 MPa in 10 MPa

increments. These simulations analyzed how variations in both soil stiffness and Poisson ratio affect the relationship, refining the model for practical application.

Stage III: Validation of Control Samples

A PLA plate with a thickness of 0.4 mm and a diameter of 49.5 mm was fabricated using a 3D printer. Both surfaces were heated to ensure smoothness, and the chosen thickness minimized deviations from the Hertz contact equation. Three rigid polyurethane foam samples, with known mechanical properties provided by the manufacturer (Sawbones Europe AB, 2002), were used to evaluate the device's ability to measure elastic properties. Additionally, simple soil samples were conducted to validate the effectiveness of the modification.

The travel time (TOF) was measured experimentally, and the Young's modulus of each material was determined using the TOF-Young modulus relationship from Stage II. These experimentally obtained values were compared to the manufacturer's specifications. Table 2 shows the TOF computed via the Stage II numerical formulation, using the sample's provided Young's modulus, alongside the experimentally measured TOF for validation.

| Manufacture ID | Young Modulus (MPa) (Sawbones Europe AB, 2002) | Poisson Ratio (-) (Marter, Dickinson, Pierron, Ki, & Browne, 2019) | TOF_{Simulation} | TOF_{Experimental} | TOF - Percentual Difference (%) |
|-----------------------|--|---|---------------------------------|-----------------------------------|--|
| PCF 08 | 38 | 0.34 | 0.00180 | 0.00178 | 1.36 |
| PCF 15 | 123 | 0.33 | 0.00146 | 0.00146 | 0.00 |
| PCF 30 | 445 | 0.30 | 0.00115 | 0.00115 | 0.03 |

Table 2-Material Properties of Control samples and experimental measurements.

The experimental setup incorporated three key electronic components for signal transfer, measurement, and processing. Stress signals were captured using a PCB Piezotronics 208C02 load cell, with an operational frequency range of 0.001 kHz to 36 kHz and a maximum load capacity of 100 lb. The load cell was directly connected to a National Instruments cDAQ-9174 data acquisition chassis equipped with a 9234 module, specifically designed for precise signal acquisition. The recorded data was processed using MATLAB on a laptop interfaced with the

DAQ system. Figure 4 illustrates the solitary strain wave device, the sensor, the data acquisition setup, and the connected computer.

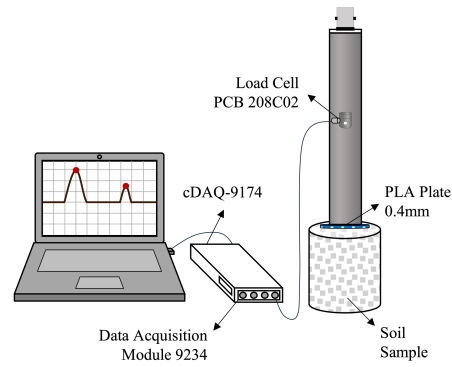


Figure 4-Solitary-Strain wave device setup.

RESULTS AND DISCUSSION

The results follow the same sequence as the methodology. The finite element analysis introduced a modified Hertz equation to account for the plate's influence, while the finite difference simulation established a relationship between TOF and the sample's Young's modulus. The device's performance was then evaluated on soil samples to confirm the elimination of plastic deformations, and in control samples to validate its measurement capacities.

Stage I: Finite Element Results

Finite element models analyzed the interactions between the soil sample, plate, and spherical element. Initially, the effect of different plate materials on the contact equation was studied. Figure 5 shows the numerical simulations for four cases: steel, PLA, aluminum, and no plate. The results revealed deviations from the Hertz equation for an indentation of 0.001 mm, with ratios of 0.28 (PLA), 1.75 (aluminum), and 2.75 (steel). Stiffer plates exhibited greater deviations from Hertzian behavior.

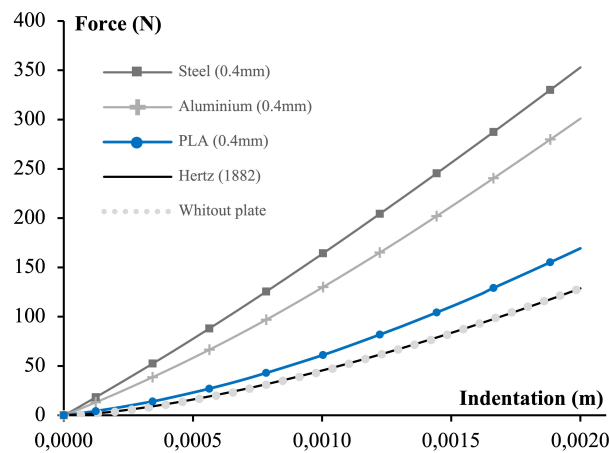


Figure 5-Indentation response of the sphere using a range of plate materials.

Among the tested materials, PLA exhibited minimal deviation and was selected for further evaluation due to its local availability. Plate thicknesses of 0.2 mm, 0.4 mm, and 1.0 mm were analyzed. Increased thickness led to greater stiffness and deviation from Hertzian behavior. For

an indentation of 0.001 mm, deviations were 37% for the 0.2 mm plate and 42% for the 0.4 mm plate, with minimal difference between these two. The 0.4 mm plate thickness was chosen for further study based on its moderate deviation and practical applicability.

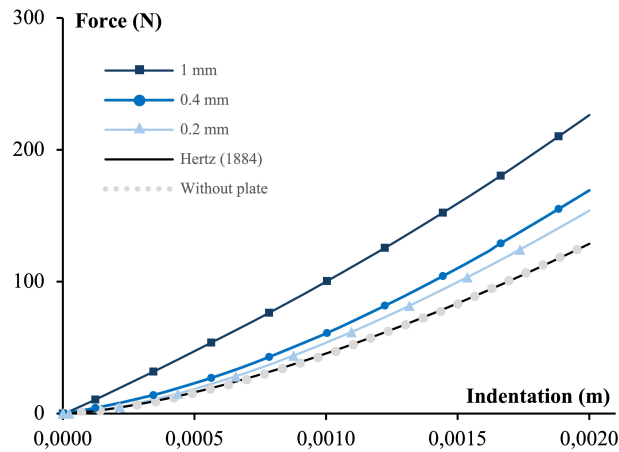


Figure 6-Indentation response of 0.0, 0.2, 0.4 and 1.0 mm PLA plates thicknesses.

Subsequent models explored the interaction of the 0.4 mm PLA plate with a metallic sphere across varying soil Young's moduli and Poisson ratios. Results were fitted to a modified Hertz equation, introducing a parameter K to capture deviations. Using ordinary least squares minimization, K was found to depend on both the soil's Young's modulus and Poisson ratio.

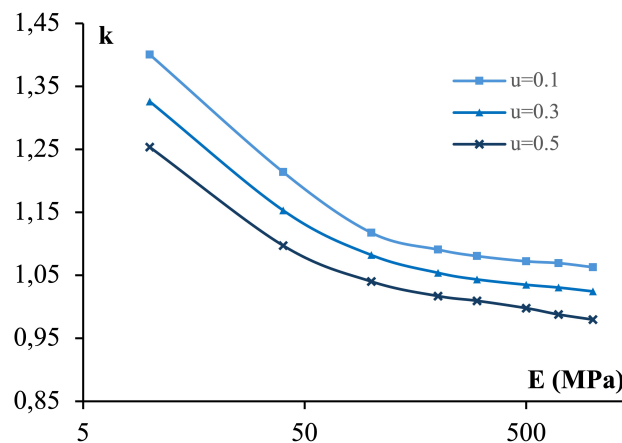


Figure 7-Fits of the FEM results to the proposed equation.

Figure 7 illustrates this relationship, showing that lower Young's modulus values amplify the plate's influence, causing greater deviation from Hertzian behavior.

Stage II: Finite difference simulation results

This section aimed to establish a relationship between the wave travel time (TOF) and the Young's modulus of the tested material. This simulation was based on the mathematical formulation developed by (Villacreses, Caicedo, Caro, & Yépez, 2021), with the primary modification being the inclusion of the parameter K , which accounts for the interaction between the last sphere, the PLA plate, and the soil. The K values obtained from Stage I were incorporated into the numerical simulation.

Figure 8 presents the relationship between TOF, measured as the time for the incident and reflected waves to travel to the sensor, and the Young's modulus of the material. The results indicate that TOF increases as the Young's modulus decreases. The impact of Poisson's ratio on TOF was found to be less significant compared to the effect of the modulus.

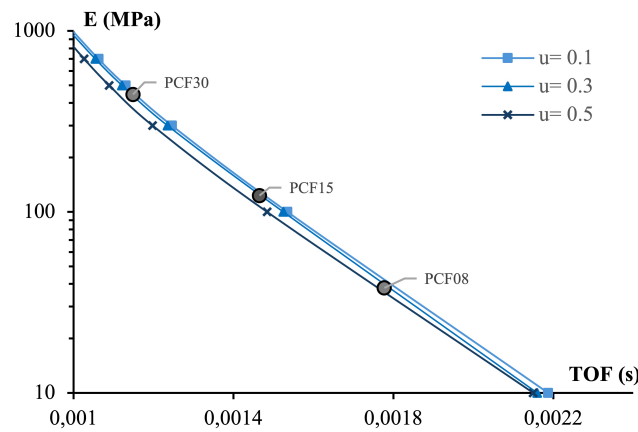


Figure 8-Relationship between Time of flight (TOF) and the Young modulus of the tested material.

This relationship enables the estimation of the Young's modulus from the measured TOF and an assumed Poisson ratio. The figure also compares TOF values measured experimentally on

control samples with the Young modulus specified by the polyurethane foam manufacturer, demonstrating consistency between the simulation and experimental results.

Stage III: Validation of Control Samples

This stage focused on two key objectives. The first was to investigate the reduction of plastic deformations that influenced the mechanical interaction of the device, affecting the experimental TOF values. The second objective was to evaluate the accuracy of Young's modulus measurements using standard control samples.

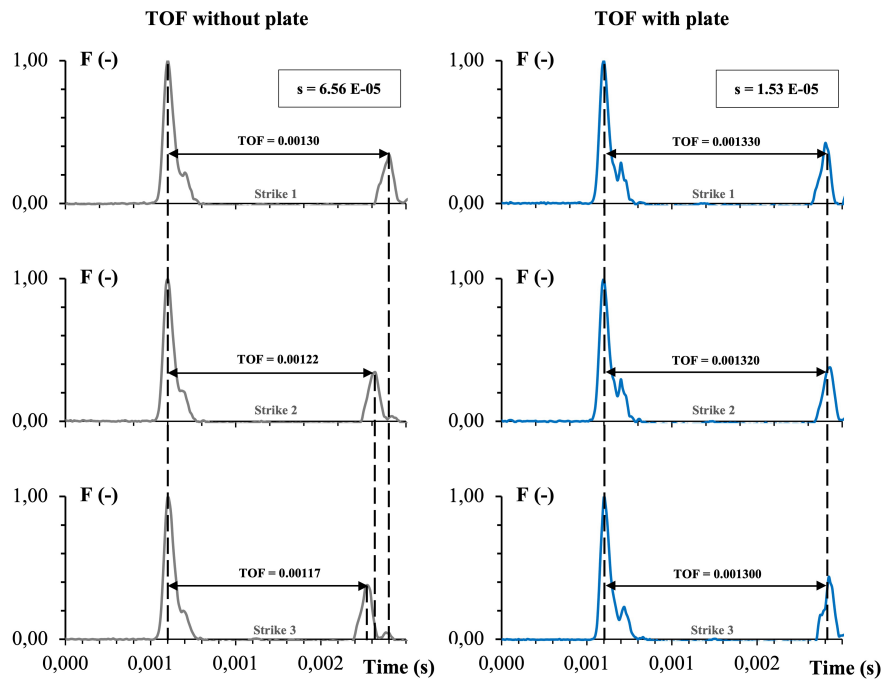


Figure 9-Unmodified and modified solitary strain wave device.

A soil sample with a density of 2.03 g/cm^3 and a moisture content of 14.31% was prepared according to the materials section and tested using both the unmodified device (as described by (Villacreses, Caicedo, Caro, & Yépez, 2021)) and the modified device proposed in this study. The results from three consecutive tests are shown in Figure 9. The standard deviation for the unmodified device was 6.56×10^{-5} seconds, which is higher than the 1.53×10^{-5} seconds

observed with the modified device. This improvement is attributed to the PLA plate, which helped distribute the contact force over a broader area, reducing variations in TOF.

After achieving consistent TOF measurements, the accuracy of the finite difference simulation was evaluated. Three rigid polyurethane foam samples were tested using the modified device, and the experimental results were compared with simulations that used the manufacturer-specified Young's modulus. Table 2 reports the percentage differences between the experimental and computed TOF, with the largest difference (1.36%) observed for the PCF-08 rigid foam, and a much smaller difference (0.03%) for the PCF-30. Figure 10 shows a comparison of the measured and computed TOF for the three foams, demonstrating a strong agreement between the experimental and simulated results.

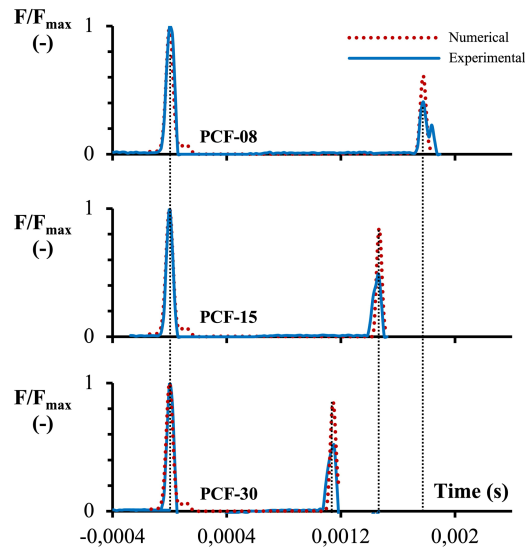


Figure 10-Comparison of measured and simulated values on rigid foam samples.

The TOF values for the polyurethane foams were then used to estimate the Young's modulus using the relationship developed in Figure 8. The estimated module was compared to the values provided by the manufacturer. The largest discrepancy between the measured and estimated modulus was found for the softest foam (PCF-08), as shown in Table 3. These results indicate

that the device's accuracy in determining Young's modulus decreases as the tested material becomes softer.

| Manufacture ID | E (MPa) | Measured E (MPa) | COV Measured E (%) | Percentual Difference (%) |
|-----------------------|--------------------|---------------------------------|-----------------------------------|--------------------------------------|
| PCF 08 | 38 | 39 | 11.07 | 3 |
| PCF 15 | 123 | 122 | 6.81 | 1 |
| PCF 30 | 445 | 442 | 7.24 | 1 |

Table 3- Measured Young modulus using de Solitary strain wave device.

CONCLUSIONS

This study highlights the potential of the modified solitary strain wave device, enhanced by the incorporation of a thin PLA plate, to improve the consistency and accuracy of Time of Flight (TOF) measurements. The modification effectively distributes contact forces, reducing plastic deformations, which is particularly beneficial for soil testing applications. The results demonstrate that the inclusion of the PLA plate leads to more consistent TOF measurements in soil compared to the unmodified device, showcasing its value for improved accuracy in field applications.

Using a finite element approach, a modified Hertz contact equation was developed, which establishes a relationship between TOF and Young's modulus, with a selected PLA plate thickness of 0.4 mm. Testing on rigid polyurethane foams revealed a strong correlation between TOF and Young's modulus, with an error margin of just 3% for PCF-08 foam and only 1% for PCF-30 foam. These results demonstrate that the modified device is highly accurate when testing harder materials, while still maintaining reliable performance with softer materials.

To further validate the effectiveness and applicability of this device, future studies should explore the use of additional materials with known Young's modulus values. Expanding the range of tested materials will help assess the device's versatility and its ability to accurately measure Young's modulus across a broader spectrum of materials. Comparing the results with other established techniques, such as conventional wave propagation methods and laboratory testing, would provide further insights into the reliability and accuracy of the modified device. Furthermore, it is essential to evaluate the feasibility of using this device in the field for real-time soil testing. Future work should assess the device's performance in field conditions. Integrating this device into practical applications like field compaction control.

BIBLIOGRAPHY

- Nesterenko, V. (2013). *Dynamics of heterogeneous materials*. Springer Science & Business Media.
- Rizzo, P., & Li, K. (2017). Analysis of the geometric parameters of a solitary waves-based harvester to enhance its power output. *Smart Materials and Structures*, 26, 75004.
- Villacreses, J. P., Caicedo, B., Caro, S., & Yépez, F. (2021). Feasibility of the use of nonlinear solitary waves for the nondestructive measurement of Young's modulus of rocks and compacted materials. *Transportation Geotechnics*, 26, 100437.
- Popov, V. L. (2010). *Contact mechanics and friction*. Springer.
- Sneddon, I. N. (1965). The relation between load and penetration in the axisymmetric Boussinesq problem for a punch of arbitrary profile. *International Journal of Engineering Science*, 3, 47–57.
- Zhai, C., Gan, Y., Hanaor, D., Proust, G., & Retraint, D. (2016). The role of surface structure in normal contact stiffness. *Experimental Mechanics*, 56, 359–368.
- Hertz, H. (1882). Ueber die Berührung fester elastischer Körper. *Journal für die reine und angewandte Mathematik*, 92, 152-171.
- Ni, X., Rizzo, P., Yang, J., Katri, D., & Daraio, C. (2012). Monitoring the hydration of cement using highly nonlinear solitary waves. *NDT & E International*, 52, 76–85.
doi:10.1016/j.ndteint.2012.05.003
- Yang, J., Silvestro, C., Khatri, D., De Nardo, L., & Daraio, C. (2011). Interaction of highly nonlinear solitary waves with linear elastic media. *Physical Review E*, 83, 46606.
- Sawbones Europe AB. (2002). Product catalogue 2002. *Product catalogue 2002*.

Marter, A., Dickinson, A., Pierron, F., Ki, Y., & Browne, M. (2019). Characterising the compressive anisotropic properties of analogue bone using optical strain measurement. *Journal of Engineering in Medicine*, 233(9), 954-960.

Belcher, D. J. (1952). *Nuclear meters for measuring soil density and moisture in thin surface layers*. Tech. rep.

Carol, M., Bernardo, C., & Luc, T. (2010). A Miniature Falling Weight Device for Non-Intrusive Characterization of Soils in the Centrifuge. 1–10.